Biophysical Chemistry 26 (1987) 83–89
Elsevier

BPC 01127

Diffusion-controlled association of a dye, 1-anilinonaphthalene-8-sulfonic acid, to a protein, bovine serum albumin, using a fast-flow microsecond mixer and stopped-flow

Peter Regenfuss and Robert M. Clegg

Abteilung Molekulare Biologie, Max-Planck-Institut für biophysikalische Chemie, Postfach 2841, D-3400 Göttingen, F.R.G.

Received 27 October 1986
Revised manuscript received 15 December 1986
Accepted 30 December 1986

Bovine serum albumin; Protein-ligand binding; Binding kinetics; Stopped-flow; Fast-flow mixer; 1-Anilinonaphthalene-8-sulfonic acid

The kinetic constants of the two fastest reactions of 1-anilinonaphthalene-8-sulfonic acid binding to bovine serum albumin are derived from the results of experiments with a microsecond fast-flow mixing technique and a stopped-flow method. The experiments are interpreted in terms of rapid bimolecular diffusion-controlled associations to two independent regions on the protein surface; this reaction mechanism contrasts with previous kinetic studies of ligand binding to bovine serum albumin which have not demonstrated the fastest kinetic processes.

1. Introduction

The equilibrium binding parameters determined for the binding of a multitude of ligands to BSA and HSA [1,2] have been instrumental in understanding the function of serum albumins and their biological role. This extensive available information, concomitant with the early and easy accessibility of these proteins, has made them useful as models to study protein-ligand interactions [1–9].

On the other hand, considerably fewer kinetic studies involving BSA and ligands have been attempted. Goldsack and Waern [10] performed pressure-jump experiments with the BSA-phenol red system to study the dynamics of conformational changes of the protein. Stopped-flow experiments [8] with HSA and warfarin have shown multiple kinetic processes in the 10–100 ms time region. No experimental confirmation of a diffusion-controlled encounter complex was obtained, but the authors assumed that this was based upon the high concentration limits of their observed relaxation times. They attributed the slow observed rates to subsequent conformational changes of the complex.

Nakatani et al. [11] have carried out stopped-flow experiments with the BSA-ANS system. They reported that the progress of the binding reaction could be accounted for by a single exponential function under first-order conditions of excess BSA. The time constant of this decay was independent of the excess reactant concentration and they could not determine any individual rate constants. However, they noticed a faster kinetic process which was too rapid to be resolved by their stopped-flow method. Based upon this evidence

Correspondence address: P. Regenfuss, Abteilung Molekulare Biologie, Max-Planck-Institut für biophysikalische Chemie, Postfach 2841, D-3400 Göttingen, F.R.G.

Abbreviations: ANS, 1-anilinonaphthalene-8-sulfonic acid; BSA, bovine serium albumin; HSA, human serum albumin.

they proposed a sequential model (bimolecular association followed by a conformational change) for ANS binding to BSA.

We have applied a new fast-flow mixing technique to observe directly the fastest binding of ANS to BSA. With this method [12] we can completely mix two aqueous solutions within 10 μs and investigate kinetic processes which are 10^3-times faster than can be seen by normal stopped-flow techniques. In addition to these very fast-flow mixing experiments we have investigated much lower reactant concentrations than Nakatani et al. [11], with a conventional, but sensitive, stopped-flow instrument. In this low concentration range we can observe a concentration-dependent time constant and determine the appropriate rate constants.

By combining the data from the very fast-flow mixer with that of the slower stopped-flow data we propose that the ANS molecules bind with a simple bimolecular association step, and that the multiple binding sites on the protein are independent. We can also estimate the size of the binding sites on the protein surface from the magnitude of the association rate constants. Contrary to all other kinetic studies of ligand binding to albumins we do not find it necessary to hypothesize a conformational change of the protein structure.

ANS has been used as a competitive fluorescent indicator in investigations of the binding of antibiotics to BSA [13,14]. ANS undergoes a large increase in fluorescence quantum yield upon binding to BSA in aqueous solution: the quantum yield increases from about 0.004 [15,16] to 0.75 and there is a slight blue shift of the maximum emission wavelength [16]. Five ANS molecules are bound per BSA protomer with pK values of 6.2–5.4 for pH values from 5 to 10, respectively [17]. At pH 7 (phosphate buffer) one binding process was an order of magnitude stronger, but the quantum yield is claimed to be identical for all five bound ANS species [17].

2. Experimental

Substances, reaction conditions and instrumentation: BSA was from Sigma (St. Louis, MO, U.S.A.; grade of purity – essentially free from fatty acids; 16% nitrogen content) ANS was from Serva (Heidelberg; crystalline magnesium salt; purity p.a.). All experiments were carried out at 25°C in 0.1 M phosphate buffer at pH 7.

The progress of the reaction was recorded by observing the fluorescence of ANS. The spectral region of fluorescence was selected with a 523 nm Schott cut-off filter. The excitation sources were either a 150 W Hg high-pressure short arc or a 200 W Hg/Xe compact arc from Hanovia. The excitation light was passed through a narrow-band 365 nm filter from Corion.

The fastest binding processes were measured with an instrument for continuous rapid mixing on a microscale, developed by us [12,18]. The time required for 100% complete mixing on a molecular scale was only 14 μs using a 0.17 ml s^{-1} flow rate, while the reaction could be conveniently observed for quantitative kinetic measurements at all times longer than 34 μs after the completion of mixing. The fluorescence of the thin jet stream ejected from the 120 μm nozzle was recorded upon a photographic film and the fluorescence was then determined densitometrically with a Joyce Loebl 3CS microdensitometer: appropriate corrections for the sensitivity of the film and intensity normalization were made [18].

The stopped-flow apparatus has been previously described [19,20]. The dead time is 2.4 ms. The data acquisition is computer controlled and all calculations were made on a DEC 11/23 minicomputer. The multiexponential analysis of the first-order kinetic progress curves has been described previously [21].

The stopped-flow experiments were carried out at BSA concentrations ($M_r = 68\,000$) between 0.1 and 1 μM and with a constant ANS concentration of 0.05 μM, after mixing. The results of eight experiments were averaged for every concentration.

3. Data analysis

The first-order stopped-flow progress curves were fitted by the nonlinear regression method of Marquardt (program written by Leon Avery) to a

sum of exponentials. The stopped-flow kinetic progress curves were dominated by a single exponential; however, much slower processes were also observed. These slower processes were of very low amplitude and much slower than the primary binding events. To account for minor deviations from a single major exponential decay within the time of 2–100 ms it was sometimes necessary to simulate two exponentials to fit the stopped-flow data. This double-exponential fit always clearly showed that the overwhelming amplitude belonged to a single major exponential process; the very slow process always had a decay time longer than the total time for data collection, the corresponding amplitude being less than 5% of the total amplitude.

The progress of the very rapid process observed in the fast-flow mixer was never observed in the stopped-flow experiment and indeed our reaction model would predict that it would always have completely decayed within the dead time of the stopped-flow measurement. The amplitude of this very rapid process was, however, always recorded as the difference between the fluorescence signal of the buffer + ANS and the fluorescence at the beginning of the major stopped-flow signal immediately after mixing this solution with BSA.

The data from the jet mixer were corrected and normalized as explained above, and the exponential kinetic progress curves were fitted using a Chebyshev transform nonlinear regression method [21].

The kinetic constants were determined by direct simulation of the data from the kinetic model equations (see section 4); the final values were selected by iteratively minimizing the total global variance.

4. Results

Fig. 1 shows a stopped-flow progress curve under first-order conditions; within this time range the curve can be fitted by one exponential time function, indicating a single kinetic process. As shown in fig. 2 the inverse of this decay time approaches a plateau value at higher protein concentrations, indicating that this kinetic process is

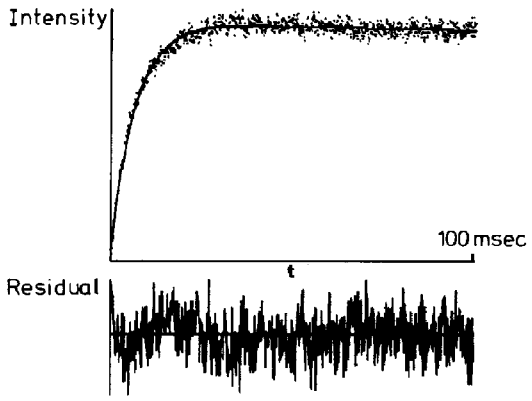

Fig. 1. Exponential fit of a stopped-flow curve (average of 8 experiments). [BSA] = 0.5 μM, [ANS] = 50 nM. See text for details.

more complex than a singular binding event. To investigate a much faster time region we applied the fast-flow mixer which allows measurements to be made 1000-times faster than can be observed by the stopped-flow method. Fig. 3 shows the result of a densitometric analysis from a photograph of the fluorescent 'jet in air' using the fast-flow mixer. The exponential fit is excellent, verifying that the kinetics measured by the fast-flow mixer is that of a single uncoupled binding process which is much more rapid than that seen in the stopped-flow measurements. The two experimental methods show two temporally well

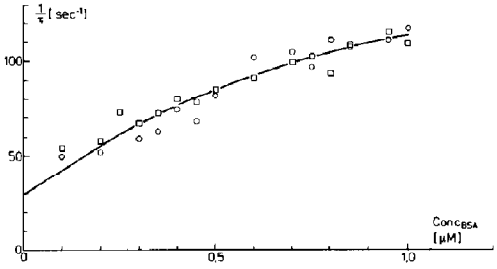

Fig. 2. Reciprocal of the stopped-flow decay times vs. the concentration of BSA which is in excess. The individual reaction progress curves are exponential due to the pseudo first-order reaction conditions ([BSA] > [ANS] = 50 nM). The solid line is the calculated expectation according to the parameters of table 1 for the 1 : 1 distribution: the fits corresponding to all the distributions are practically indistinguishable.

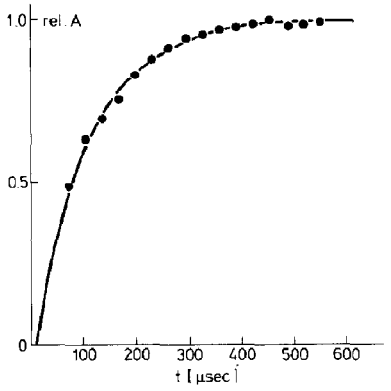

Fig. 3. Recording of the reaction of BSA (4 μM) and ANS (20 μM) in 0.1 M phosphate (pH 7) at 22°C in the fast-flow mixing experiment. (●) Experimental results obtained by evaluating corrected and calibrated absorbance curves of the photographically recorded fluorescent continuous flow. The fitted exponential decay time (———) is 104 μs giving an equivalent bimolecular forward rate constant of about 5×10^8 M^{-1} s^{-1} under the assumption that the dissociation rate constant does not contribute significantly and that the reaction is solely related to an independent fast binding site on the BSA for ANS.

separated kinetic processes and the concentration dependence of the stopped-flow results indicate that the two processes are coupled by dependent chemical reactions.

The simplest mechanism accounting for the data consists of two parallel bimolecular binding events. Two types of binding sites, B_1 and B_2 on the protein, are assumed to be independent, thermodynamically and spectroscopically: the two reaction steps are coupled only by the common ligand, A.

$$\begin{aligned} &A + B_1 \underset{k_{-1}}{\overset{k_1}{\rightleftharpoons}} C_1 \qquad A = \text{ANS} \\ &\qquad\qquad\qquad\qquad B_1, B_2 = \text{BSA-binding sites} \\ &A + B_2 \underset{k_{-2}}{\overset{k_2}{\rightleftharpoons}} C_2 \qquad C_1, C_2 = \text{complexes} \end{aligned} \tag{1}$$

Since all the stopped-flow measurements were made with BSA in excess, the solution of the kinetic differential equations is a series of exponentials, which in column vector notation reads:

$$\begin{bmatrix} [C_1]_t \\ [C_2]_t \end{bmatrix} = \beta_1 \begin{bmatrix} \Delta_1^1 \\ \Delta_2^1 \end{bmatrix} e^{-t\lambda_1} + \beta_2 \begin{bmatrix} \Delta_1^2 \\ \Delta_2^2 \end{bmatrix} e^{-t\lambda_2} + \begin{bmatrix} [C_1]^\infty \\ [C_2]^\infty \end{bmatrix} \tag{2}$$

$[C_i]^\infty$ is the infinite time equilibrium concentration of the complexes. β_i and λ_i are the amplitude and apparent kinetic constant of the i-th normal mode of the progress curve, and Δ_j^i the jth components of the i-th normalized eigenvector of the homogeneous system of differential equations.

The general solution to these first-order equations is algebraically complex: however, anticipating the results given below we note that even if the two reactions have similar bimolecular association rate constants, the measured rates of the two-exponential progress curves can differ considerably if the dissociation rates are significantly different. Actually, at very low reactant concentrations, but still under first-order conditions, $\lambda_1 \approx k_{-1}$ and $\lambda_2 \approx k_{-2}$. All four rate constants can be determined from a global fit of the concentration

Table 1

Kinetic and equilibrium constants of the two fastest reaction steps on the assumption of a parallel mechanism using three ratios $P_2^0 : P_1^0$ of the total binding sites on the protein of the two types

We estimate the accuracy of the rate constants to be between ±20%

$P_2^0 : P_1^0$	k_1 (M^{-1} s^{-1})	k_{-1} (s^{-1})	k_2 (M^{-1} s^{-1})	k_{-2} (s^{-1})	K_I (M^{-1})	K_{II} (M^{-1})
1:1	5.0×10^8	7.0×10^2	1.5×10^8	3.0×10^1	7.1×10^5	5.0×10^6
2:3	3.7×10^8	1.0×10^3	9.3×10^7	2.7×10^1	3.7×10^5	3.4×10^6
1:4	3.2×10^8	1.2×10^3	2.0×10^8	2.2×10^1	2.8×10^5	9.1×10^6

dependence of the two-exponential fits.

The fast-flow experiments were performed with [ANS] > [BSA] so that $\lambda_1 \approx (k_1 + k_2)$([ANS]) (and $\lambda_1 \gg k_{-1}$; see below). This assumption for parameter estimates is consistent with the final results in table 1. The data were fitted to the exact quadratic solution of the linearized kinetic equation with no assumption except for the first-order condition. The sets of rate constants which are globally consistent with the fast-flow mixer, stopped-flow curves and known equilibrium constants are listed in table 1. There are five ANS molecules bound to each BSA protomer at saturation. Since we do not know a priori how the molecular binding sites are partitioned between the two binding regions corresponding to the fast and slow kinetic processes, we have fitted the data to the model of eq. 1 assuming the following conditions for the ratio of total sites on each protein: $P_2^0 : P_1^0 = 1:4$ or $2:3$ or $1:1$ (fig. 2 shows the fit for the ratio of 1 : 1). That is, either there are more sites binding with a rate constant of k_1 than sites with a rate constant of k_2, with a ratio of 1 : 4 or 2 : 3; or the sites are 'formally' equally partitioned, with a ratio of 1 : 1. As shown in table 1, the rate constants do depend upon the site partitioning selected, but not very much; even for the case of a 1 : 1 ratio, the fitted rate constants are similar to those for the other ratios. For all these choices we still conclude that the BSA molecule has two binding regions which differ mainly in the dissociation rate constants. The data can be accounted for equally well by all partitioning choices.

The amplitudes of the stopped-flow curves directly yield information about the slow process, which is within the time range available to this method. Since we know the fluorescence intensity of the separate reactants before they react, we can determine the amplitude of the faster reaction which has reached completion before the dead time of the stopped-flow experiment. This fast process is that seen with the fast-flow mixing method. Fig. 4 is a schematic illustration of the separate contributions to the total amplitude of a stopped-flow experiment. Not only does the concentration dependence of these amplitudes give an independent check upon the rate and equilibrium constants determined from the decay times in table 1, but we can also calculate the relative quantum yields of ANS at the separate occupied binding sites on BSA. The quantum yield of ANS bound to the faster binding region ('1') is shown

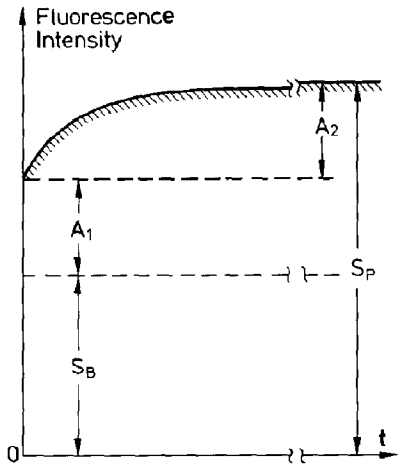

Fig. 4. Representation of the total measured stopped-flow fluorescence; A_1, signal of the fastest exponential which has decayed completely within the dead time of the stopped-flow; A_2, kinetic process measured with the stopped-flow; S_P, total measured signal after time t; S_B, fluorescence signal of the corresponding initial BSA and ANS concentrations in buffer.

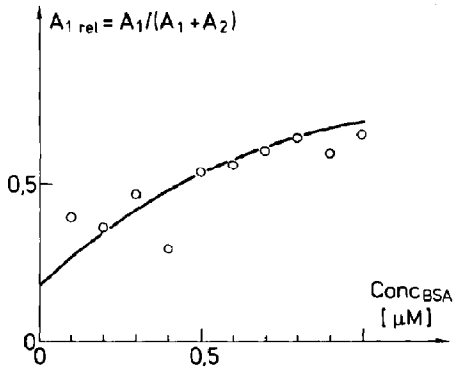

Fig. 5. The relative amplitude of the fastest kinetic process, A_1 rel $= A_1/(A_1 + A_2)$ (see fig. 4 for symbols), increases as the BSA concentration is increased (constant [ANS]). The solid line represents the fit to our data (O) for our kinetic model, provided that the fluorescence quantum yield of the most rapidly formed complex is 75% of that for the more slowly formed complex and there are only two reacting sites on the protein.

to be 75% of that of the slower binding region ('2') assuming a 1 : 1 ratio of $P_2^0 : P_1^0$. In fig. 5 we have plotted the relative amplitudes as explained in the legend.

5. Discussion

In spite of the very rapid bimolecular rate constants of $1.5–5 \times 10^8$ M^{-1} s^{-1}, these rates are still an order of magnitude smaller than one would expect for a spherically symmetric diffusion-controlled association. The expected bimolecular rate constant for a diffusion-controlled encounter of an equivalent sphere with a diameter of a BSA protomer and a small molecule like ANS is [24],

$$k_f = \frac{4\pi}{1000} N_A R_{AB} D_{AB} \qquad (3)$$

R_{AB} is the minimal distance of separation between the centers of the protein and the ligand (assuming both to be spheres): $R_{AB} = R_A + R_B$, where R_A and R_B are the radii of the two reactant molecules. The diffusion constant for the relative motion of both reactants (i.e., BSA and ANS) is D_{AB} and N_A is Avogadro's number. If $D_{AB} \cong 3 \times 10^{-6}$ cm^2 s^{-1} and $R_{AB} \simeq 25$ Å this equation predicts an association rate constant of 6×10^9 M^{-1} s^{-1} which is 10-times that which we measure. This leads us to the conclusion that ANS associates with only a fraction of the total surface area of the protein; i.e., the total protein surface is not available for interaction with ANS. If the reaction is diffusion controlled, i.e., every molecular encounter of the reaction partners produces a complex, we can estimate the size of the reactive area on the protein surface by the following arguments (ref. 24 and references therein).

For the case where the ligand is much smaller than the protein, and the linear dimension of the site is much smaller than the protein radius, a good estimate of the rate of bimolecular association is

$$k_f = \frac{4\pi N_A}{1000} R_{AB} D_{AB} (\sin(\theta/2)) \qquad (4)$$

where θ is the solid angle representing the angular extension of a circular site boundary, measured from the center of the large protein sphere. Since our measured association rates are about a factor of 10 smaller than the diffusion-controlled prediction of eq. 3, we have $\sin(\theta/2) \cong 0.1$, which means that the reactive area of one site on the protein surface is approx. 1/100 of the total surface area of the protein. Note that this dependence of a diffusion controlled reaction upon the target size on the protein is related to the determined association rate constant, and as such is independent of the number of sites on each protein molecule. That is, the forward rate constant is ascribed to each of the individual equivalent sites; the number of sites is only important for the numerical determination of the rate constant. The total surface area of the BSA protein is about 100-times the area of the ANS conjugated ring system, and thus it is plausible that the reactive area of a binding site on the protein surface accomodates a single, or only a few, ANS molecules.

The sites on the protein are probably available to the solvent, and the kinetics very likely represent the maximum rate at which small aromatic molecules react directly with limited hydrophobic regions on protein surfaces. We note that this argument holds for both reactions of eq. 1 since the forward rates are only maximally a factor of four different. Even if the nature of the attraction is relatively nonspecific, such as hydrophobic bonding, it is still reasonable to conclude that the association rate of bimolecular binding to the rapid site is completely diffusion controlled and binds to a single distinct region on the surface of the protein. On the other hand, the difference in dissociation rates between the two reactions is much larger, about a factor of 20, and this accounts for the higher affinity of one type of binding region on the protein for ANS and the large temporal separation of the two reaction modes. The higher affinity of the region with the slowest dissociation rate constant indicates that additional attractive interactions for ANS are available in this region.

If all the sites have almost identical quantum yields, and if each site reacts according to a simple one-step bimolecular mechanism, than at higher concentrations where [BSA] ≫ [ANS] and [BSA]

≫ all the equilibrium dissociation constants, the fastest observable time constant will have an amplitude corresponding almost to the total expected binding amplitude. Subsequent kinetic observables will have low amplitudes in comparison unless one (or some) of the sites have noticeably different quantum yields. This is because at high protein (i.e., binding site) concentrations the ANS ligand will initially distribute among the sites according to the ratio of the forward rate constants, and the subsequent kinetic normal modes correspond to a reshuffling to form the final equilibrium configuration of bound species, which is dictated by the relative equilibrium constants. A redistribution of totally bound species between bound sites with identical quantum yields will exhibit no observable fluorescence change. Fig. 4 indicates that the quantum yields differ by no more than 25% and therefore, within the uncertainties of comparing our kinetic results, with the equilibrium determinations of Weber and Daniel [17], the relative amplitudes of fig. 5 support their conclusion that all the ANS-binding sites on BSA form complexes with very similar quantum yields.

To summarize, our stopped-flow observations have been made at much lower concentrations of reactants than previous studies [11], and we have measured the time course of an extremely rapid kinetic process which cannot be observed with the stopped-flow technique, by applying our fast-flow mixer. Since we have directly observed the fastest binding process we interpret the BSA-ANS reaction by means of a reaction scheme very different from the sequential model proposed by Nakatani et al. [11]. We consider it very likely that there are no major conformational changes of the BSA molecule, and that ANS binds to two restricted regions of the BSA molecule comprising totally only a few percent of the protein surface area. The association rates are diffusion controlled and similar for the two regions: the difference between the affinities of the two binding regions is mainly due to the dissociation rates. The bimolecular association rates are among the fastest that have been measured for protein-ligand interactions [22,23].

Acknowledgements

We gratefully acknowledge Dr. P. Mitra for careful reading and constructive comments on the manuscript and Dr. T.M. Jovin for support and encouragement of the project.

References

1 U. Kragh-Hansen, Pharmacol. Rev. 33 (1981) 17.
2 J.R. Brown and P. Shockley, in: Lipid-protein interactions, vol. 1, eds. P. Jost and O.H. Griffith (Wiley, New York, 1982) p. 25.
3 G. Weber, Adv. Protein Chem. 29 (1975) 1.
4 M.T. Flanagan and S. Ainsworth, Biochim. Biophys. Acta 168 (1968) 16.
5 J.E. Fletcher and A.A. Spector, Mol. Pharmacol. 13 (1977) 387.
6 G.M. Edelman and W.L. McClure, Acc. Chem. Res. 1 (1968) 65.
7 B. Witholt and L. Brand, Biochem. 9 (1970) 1948.
8 A. Lassmann and N. Rietbrock, in: Studies in physical and theoretical chemistry 26: Aggregation processes in solution, eds. E. Wyn-Jones and J. Gormally (Elsevier, Amsterdam, 1983) p. 383.
9 T. Peters, Jr., in: Advances in protein chemistry, eds. C.B. Afinsen, J.T. Edsall and F.M. Richards (Academic Press, London, 1985) p. 161.
10 D.E. Goldsack and P.M. Waern, Can. J. Biochem. 49 (1971) 1267.
11 H. Nakatani, M. Haga and K. Hiromi, FEBS Lett. 43 (1974) 293.
12 P. Regenfuss, R.M. Clegg, M.R. Fulwyler, T.M. Jovin and F.J. Barrantes, Rev. Sci. Instrum. 56 (1985) 283.
13 P.L. Hsu, J.K.H. Ma, H.W. Jun and L.A. Luzzi, J. Pharm. Sci. 63 (1974) 27.
14 P.L. Hsu, J.K.H. Ma and L.A. Luzzi, J. Pharm. Sci. 63 (1974) 570.
15 G. Weber and L.B. Young, J. Biol. Chem. 239 (1964) 1415.
16 D.C. Turner and L. Brand. Biochemistry 7 (1968) 3381.
17 G. Weber and E. Daniel, Biochemistry 5 (1966) 1893.
18 P. Regenfuss, Ph.D. Thesis, Universität Erlangen-Nürnberg, F.R.G. (1985).
19 T.M. Jovin, in: Concepts of biochemical fluorescence, eds. R. Chen and H. Edelhoch (M. Dekker, New York, 1975) p. 305.
20 A. van Landschoot, F.G. Loontiens, R.M. Clegg and T.M. Jovin, Eur. J. Biochem. 103 (1980) 313.
21 H. De Boeck, R.B. Macgregor, Jr, R.M. Clegg, N. Sharon and F.G. Loontiens, Eur. J. Biochem. 149 (1985) 141.
22 M. Eigen, in: Quantum statistical mechanics in the natural sciences, eds. B. Kursunoglu, S.L. Mintz and S.M. Widmayer (Plenum Press, New York, 1974) p. 37.
23 G.G. Hammes and P.R. Schimmel, in: The enzymes, kinetics and mechanism II, 3rd edn. ed. P.D. Boyer (Academic Press, London, 1970) p. 109.
24 O.G. Berg and P.H. von Hippel. Annu. Rev. Biophys. Chem. 14 (1985) 131.